

Throughput Performance of CF-Based Adaptive PAPR Reduction Method for Eigenmode MIMO-OFDM Signals with AMC

Shoki Inoue and Kenichi Higuchi

Graduate School of Science and Technology
Tokyo University of Science

2641 Yamazaki, Noda, Chiba 278-8510 Japan

E-mail: j7311612@ed.noda.tus.ac.jp, higuchik@rs.noda.tus.ac.jp

Teruo Kawamura

Radio Access Network Development Department
NTT DOCOMO, INC.

3-5 Hikari-no-oka, Yokosuka, Kanagawa 239-8536 Japan

E-mail: kawamura@nttdocomo.com

Abstract—This paper proposes an enhancement to a previously reported adaptive peak-to-average power ratio (PAPR) reduction method based on clipping and filtering (CF) for eigenmode multiple-input multiple-output (MIMO) - orthogonal frequency division multiplexing (OFDM) signals. We enhance the method to accommodate the case with adaptive modulation and channel coding (AMC). Since the PAPR reduction process degrades the signal-to-interference and noise power ratio (SINR), the AMC should take into account this degradation before PAPR reduction to select accurately the modulation scheme and coding rate (MCS) for each spatial stream. We use a lookup-table-based prediction of SINR after PAPR reduction, in which the interference caused by the PAPR reduction is obtained as a function of the stream index, frequency block index, clipping threshold for PAPR reduction, and input backoff (IBO) of the power amplifier. Simulation results show that the proposed PAPR reduction method increases the average throughput compared to the conventional CF method for a given adjacent channel leakage power ratio (ACLR) even when we assume AMC.

I. INTRODUCTION

The combination of orthogonal frequency division multiplexing (OFDM) and multiple-input multiple-output (MIMO) transmission is a promising modulation/radio access scheme for future wireless communication systems, e.g., the long term evolution (LTE) system in the 3rd Generation Partnership Project (3GPP) [1], since frequency efficiency in a multipath fading channel can be significantly enhanced using simple transceiver structures. In MIMO-OFDM transmission, precoding based on the channel knowledge at the transmitter enhances the MIMO capability. In particular, the eigenmode precoding based on the singular value decomposition (SVD) of the channel matrix (hereafter eigenmode MIMO) [2] is known to achieve the channel capacity.

One of the major drawbacks of the OFDM signal based on multicarrier transmission is the high peak-to-average power ratio (PAPR) of the transmission signal. Due to this high PAPR, the OFDM signal requires a large input backoff (IBO) at the transmit power amplifier and this results in inefficient power conversion and reduced average transmission power relative to that for a single-carrier transmission. A number of PAPR reduction techniques have been proposed. In this paper, we focus on the PAPR reduction techniques that do not require side information [3-8]. The clipping and filtering (CF) method [4, 5] limits the peak envelope of the input signal in the time domain to a predetermined value. The CF method is very effective in reducing the PAPR and does not reduce the

frequency efficiency; however, it causes in-band interference due to the peak reduction signal [9]. In [10] to [12], PAPR reduction problems in MIMO-OFDM are discussed. References [10] and [11] assume no precoding. Reference [12] assumes eigenmode MIMO and applies the selected mapping (SLM) [13] and partial transmit sequence (PTS) [14] method.

When we consider the application of CF to the precoded MIMO signal at each antenna, each of the transmission data streams experiences interference due to the added peak reduction signal. However, in general, the impact of the interference on the channel capacity is dependent on the equivalent channel conditions of the streams. Therefore, members of our group proposed a new PAPR reduction method based on CF of the precoded MIMO-OFDM signal to minimize the capacity degradation due to the interference caused by the peak reduction signal [15]. The main idea of this method is to prevent the application of high-power interference to the streams that experience good channel conditions based on an iterative algorithm. Although the proposed method is applicable to any kind of precoding scheme, we focus on the application of the method to the eigenmode MIMO transmission in this paper.

In [15] and [16], it is shown that our previously reported method achieves a better tradeoff between the PAPR and capacity compared to the conventional CF method assuming ideal Gaussian modulation. However, in a real system, e.g., in [1], the combination of quadrature amplitude modulation (QAM) and channel coding such as turbo coding is used and adaptive modulation and channel coding (AMC) controls the set comprising the modulation scheme and coding rate (MCS) according to the received signal-to-interference and noise power ratio (SINR). Furthermore, the final performance measure should be the achievable throughput versus the adjacent channel leakage power ratio (ACLR) [22]. Therefore, this paper proposes an enhancement to the previously reported adaptive PAPR reduction method to accommodate the case with AMC using QAM and a variable rate turbo code. Since the PAPR reduction process degrades the SINR, the AMC should take into account this degradation before PAPR reduction for accurate selection of the MCS for each spatial stream. To achieve this, we apply a lookup-table-based prediction of the SINR after PAPR reduction. For the ACLR measurement, we employ the Rapp model [19] as a non-linearity model of the power amplifier.

The remainder of the paper is organized as follows. First, Section II briefly describes the eigenmode MIMO-OFDM transmission and our previously reported PAPR reduction method. Section III describes the AMC method with the

prediction of the SINR after PAPR reduction and the Rapp model. Section IV presents simulation results that show the tradeoff between the achievable ACLR and the throughput. Finally, Section V concludes the paper.

II. EIGENMODE MIMO-OFDM TRANSMISSION AND ADAPTIVE PAPR REDUCTION METHOD

A. Eigenmode MIMO-OFDM Transmission

This section briefly describes the eigenmode MIMO-OFDM transmission based on the SVD of the channel matrix [2]. We consider MIMO multiplexing with N_{tx} transmitter antenna branches and N_{rx} receiver antenna branches. The number of streams, L , which are spatially multiplexed, is set to N_{tx} . It should be noted that among $L = N_{tx}$ streams, the number of streams eventually used for information data transmission is equal to or less than $N_{min} = \min(N_{tx}, N_{rx})$. The number of frequency blocks, in each of which different fading is observed, is B . The number of subcarriers per frequency block is K . We denote the $K \times 1$ -dimensional frequency-domain OFDM signal vector of the l -th ($1 \leq l \leq L$) stream at the b -th ($1 \leq b \leq B$) frequency block as $\mathbf{c}_{b,l}$.

Assuming that \mathbf{H}_b is the $N_{rx} \times N_{tx}$ -dimensional channel matrix at the b -th frequency block, \mathbf{H}_b can be SVD decomposed as

$$\mathbf{H}_b = \mathbf{U}_b \mathbf{\Lambda}_b \mathbf{V}_b^H, \quad (1)$$

where \mathbf{U}_b is the $N_{rx} \times N_{rx}$ -dimensional unitary matrix and \mathbf{V}_b is the $N_{tx} \times N_{tx}$ -dimensional unitary matrix. Term $\mathbf{\Lambda}_b$ is the $N_{tx} \times N_{tx}$ -diagonal matrix with nonnegative real numbers on the diagonal, which represents the l -th singular value, $\lambda_{b,l}$, for the b -th frequency block.

$$\mathbf{\Lambda}_b = \begin{bmatrix} \mathbf{\Sigma}_b & \mathbf{0} \\ \mathbf{0} & \mathbf{0} \end{bmatrix}, \quad \mathbf{\Sigma}_b = \text{diag}\{\lambda_{b,l}\} \quad (2)$$

Here, $\mathbf{\Sigma}_b$ is the $N_{min} \times N_{min}$ -dimensional diagonal matrix. For l of greater than N_{min} , $\lambda_{b,l}$ is zero; otherwise, we assume $\lambda_{b,l} \geq \lambda_{b,l+1}$. By performing precoding using \mathbf{V}_b at the transmitter and linear-filtering using \mathbf{U}_b^H at the receiver for the b -th frequency block, the MIMO channel transmission is transformed into BL parallel channels. Thus, the eigenmode MIMO transmission is achieved.

Waterfilling-based power allocation to the BL streams is performed using $\lambda_{b,l}$. The transmission power to the l -th stream at the b -th frequency block, $p_{b,l}$, is determined as

$$p_{b,l} = \left(w - \frac{N_0}{|\lambda_{b,l}|^2} \right)^+, \quad (3)$$

where function $(a)^+$ is equal to a if a is positive and zero if a is negative. Term N_0 is the noise power and w is determined so that the sum of $p_{b,l}$ is equal to the maximum allowable transmission power. The power controlled $K \times 1$ -dimensional frequency-domain transmission signal vector of the l -th stream at the b -th frequency block, $\mathbf{x}_{b,l}$, is represented as

$$\mathbf{x}_{b,l} = \sqrt{p_{b,l}} \mathbf{c}_{b,l}. \quad (4)$$

It should be noted that according to the power allocation, some of the streams may not be allocated transmission power

depending on the channel conditions. In this case, the effective number of streams is even lower than N_{min} . In the following, the $L \times K$ -dimensional transmission signal matrix whose (l, i) -th component represents the transmission signal from the l -th stream at the i -th subcarrier of the b -th frequency block is denoted as $\mathbf{X}_b = [\mathbf{x}_{b,1} \dots \mathbf{x}_{b,L}]^T$.

B. CF-Based Adaptive PAPR Reduction Method

Let \mathbf{Y}_b be the $N_{tx} \times K$ -dimensional frequency-domain transmission signal matrix after precoding for which the (t, i) -th component represents the transmission signal from the t -th ($1 \leq t \leq N_{tx}$) antenna at the i -th subcarrier of the b -th frequency block. Matrix \mathbf{Y}_b is obtained as

$$\mathbf{Y}_b = \mathbf{V}_b \mathbf{X}_b. \quad (6)$$

We denote $\mathbf{y}_{b,t}$ as the t -th row vector of \mathbf{Y}_b , which represents the frequency-domain transmission signal vector after precoding at the t -th antenna of the b -th frequency block. Assuming that the number of fast Fourier transform (FFT) points is F , the $F \times 1$ -dimensional time-domain OFDM signal vector at the t -th antenna, \mathbf{z}_t , is obtained as

$$\mathbf{z}_t = \text{IFFT}_F([\mathbf{y}_{1,t} \dots \mathbf{y}_{B,t} \mathbf{0}_{F-BK}]^T), \quad (7)$$

where $\mathbf{0}_{F-BK}$ is the zero vector with the length of $F-BK$. It may be noted that for a sufficiently accurate peak power measurement, F should be approximately four-times larger than BK [18].

By performing CF operations on \mathbf{z}_t , it is assumed that \mathbf{z}_t is converted to $\tilde{\mathbf{z}}_t$. Since the CF operations cause the interference, $\tilde{\mathbf{Y}}_b$ which is \mathbf{Y}_b after the CF operation can be represented as

$$\tilde{\mathbf{Y}}_b = \mathbf{Y}_b + \mathbf{\Delta}_b, \quad (8)$$

where $\mathbf{\Delta}_b$ is the $N_{tx} \times K$ -dimensional matrix representing the interference caused by the CF operations. This means that the transmission signal before precoding \mathbf{X}_b is converted as

$$\begin{aligned} \tilde{\mathbf{X}}_b &= \mathbf{V}_b^H \tilde{\mathbf{Y}}_b = \mathbf{X}_b + \mathbf{V}_b^H \mathbf{\Delta}_b = \mathbf{X}_b + \mathbf{W}_b, \\ \mathbf{W}_b &= [\mathbf{w}_{b,1} \dots \mathbf{w}_{b,L}]^T \end{aligned} \quad (9)$$

where $\mathbf{w}_{b,l}$ is the interference vector observed at the l -th stream of the b -th frequency block.

Assuming that the interference power caused by the PAPR reduction to the l -th data stream at the b -th frequency block is $I_{b,l} (= E_i[|w_{b,l,i}|^2])$, the throughput is represented as

$$C = \frac{1}{B} \sum_{b=1}^B \sum_{l=1}^L \log_2(1 + \text{SINR}_{b,l}), \quad (10)$$

$$\text{SINR}_{b,l} = \frac{|\lambda_{b,l}|^2 p_{b,l}}{|\lambda_{b,l}|^2 I_{b,l} + N_0}, \quad (11)$$

where N_0 is the receiver noise power. Equation (10) indicates that the capacity degradation is more significant for a stream with a larger $\lambda_{b,l}$ value.

To mitigate the capacity reduction due to interference caused by the CF operations, we have reported the CF-based adaptive PAPR reduction method [15]. The main idea of this method is to prevent imparting high power interference to the streams that experience good channel conditions based on an

iterative algorithm. In the method, the interference power is concentrated on the most inefficient stream(s). Let $L_{eff,b}$ be the number of streams that have a $p_{b,l}$ value greater than zero at the b -th frequency block. Then, if $L_{eff,b}$ is less than L , we can use the remaining $L - L_{eff,b}$ streams at the b -th frequency block for the purpose of only reducing the PAPR without loss of capacity assuming that we can allocate all the interference caused by the CF operations on these streams. When $L_{eff,b}$ is equal to L , we need to allow some capacity degradation, but the degradation can be alleviated compared to the conventional CF method if most of the interference power is allocated to the streams that have lower $p_{b,l}$ ($\lambda_{b,l}$) values. In the paper, we assume that when $L_{eff,b}$ is equal to L , the $L_{eff,b}$ -th stream, which has the minimum $\lambda_{b,l}$ value at the b -th frequency block, is used for PAPR reduction. Thus, in the method, the interference signal is concentrated on the $L_{pr,b}+1$ to L -th streams at the b -th frequency block, where $L_{pr,b}$ is defined as

$$L_{pr,b} = \begin{cases} L_{eff,b}, & \text{if } L_{eff,b} < L \\ L_{eff,b} - 1, & \text{otherwise} \end{cases}. \quad (12)$$

The method can be implemented using the iterative CF and interference restriction in the stream domain as shown in Fig. 1.

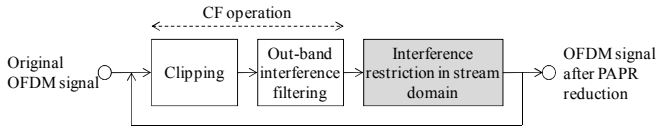


Figure 1. Block diagram of iterative algorithm for adaptive PAPR reduction method.

The following specific algorithm is applied in the paper.

Step 1) Initial setting

- ✓ Iteration index $j := 1$.
- ✓ \mathbf{X}_b is generated based on $\mathbf{c}_{b,l}$ s and $p_{b,l}$ s.
- ✓ $\hat{\mathbf{X}}_b^{(j)} := \mathbf{X}_b$.

Step 2) Precoding

- ✓ $\hat{\mathbf{Y}}_b^{(j)} := \mathbf{V}_b \hat{\mathbf{X}}_b^{(j)}$.

Step 3) CF operation

- ✓ $\hat{\mathbf{z}}_t^{(j)} := \text{IFFT}_F([\hat{\mathbf{y}}_{1,t}^{(j)} \cdots \hat{\mathbf{y}}_{B,t}^{(j)} \mathbf{0}_{F-BK}]^T)$ where $\hat{\mathbf{y}}_{b,t}^{(j)}$ is the t -th row vector of $\hat{\mathbf{Y}}_b^{(j)}$.
- ✓ Perform clipping operation on $\hat{\mathbf{z}}_t^{(j)}$ for $t = 1, \dots, N_{tx}$.
- ✓ Perform filtering operation on the clipped signal. In the paper, we assume perfect removal of the out-of-band radiation caused by the clipping using the FFT.
- ✓ After the CF operations, $\hat{\mathbf{Y}}_b^{(j)}$ is converted as $\tilde{\mathbf{Y}}_b^{(j)} = \hat{\mathbf{Y}}_b^{(j)} + \mathbf{\Lambda}_b^{(j)}$.

Step 4) Calculation of the clipped and filtered transmission signal vector before precoding

- ✓ $\tilde{\mathbf{X}}_b^{(j)} := \mathbf{V}_b^H \tilde{\mathbf{Y}}_b^{(j)}$.

Step 5) Restoration of the zero interference constraint for the $1 \sim L_{pr,b}$ -th streams

$$\checkmark \quad \mathbf{W}_b^{(j)} = \begin{bmatrix} \mathbf{I}_{L_{pr,b}} & \mathbf{0} \\ \mathbf{0} & \mathbf{0} \end{bmatrix} \hat{\mathbf{X}}_b^{(j)} + \begin{bmatrix} \mathbf{0} & \mathbf{0} \\ \mathbf{0} & \mathbf{I}_{L-L_{pr,b}} \end{bmatrix} \tilde{\mathbf{X}}_b^{(j)} - \hat{\mathbf{X}}_b^{(j)}, \quad \text{where}$$

\mathbf{I}_m is the $m \times m$ -dimensional identity matrix.

- ✓ Update of the transmission signal vector.

$$\hat{\mathbf{X}}_b^{(j+1)} := \hat{\mathbf{X}}_b^{(j)} + \mu^{(j)} \mathbf{W}_b^{(j)}$$

Step 6) $j := j + 1$. Return to Step 2.

Here, $\mu^{(j)}$ is a non-negative parameter called the gradient step size, which takes a common value for all frequency blocks. Term $\mu^{(j)}$ is determined as in [17]. The above process is repeated until the peak power is sufficiently reduced or the number of iterations reaches the maximum allowable number.

III. POWER AMPLIFIER MODEL AND AMC METHOD

A. Nonlinear Power Amplifier Model

We use the Rapp model [19] in the paper because it is a widely accepted power amplifier amplitude modulation/amplitude modulation (AM/AM) conversion model. In the Rapp model, the relationship between the time-domain input signal, $x(t)$, and the output signal, $y(t)$, of the power amplifier is represented as

$$y(t) = G_0 \frac{x(t)}{(1 + (|x(t)|/A_{SAT})^{2p})^{1/2p}}, \quad (13)$$

where G_0 is the amplifier gain in the linear transform region, A_{SAT} is the input saturating amplitude, and p is a parameter that controls the smoothness of the transition from the linear region to the saturation region. In the paper, we set $G_0 = 1$, $A_{SAT} = 1$, and $p = 2.0$ [20, 21]. To control the tradeoff between the output power and signal distortion levels in the power amplifier, the IBO is parameterized in the following evaluation. The IBO is defined as $10 \times \log_{10}(A_{SAT}^2/P_{IN})$ (dB), where P_{IN} is the mean power of the input signal before PAPR reduction. We assume ideal amplitude modulation/phase modulation (AM/PM) conversion in the paper.

B. AMC Considering Interference Due to PAPR

The AMC controls the MCS for the respective streams according to the receiver SINR for throughput maximization. The receiver instantaneous SINR in (11) can be rewritten as

$$\text{SINR}_{b,l} = \frac{S_{b,l}}{I_{b,l} + N_0} = \frac{1}{\text{ISR}_{b,l} + \text{SNR}_{b,l}^{-1}}, \quad (14)$$

$$\text{ISR}_{b,l} = I_{b,l} / S_{b,l}$$

where $S_{b,l}$ is the instantaneous received signal power of the l -th stream at the b -th frequency block, and N_0 is the receiver noise power (possibly including co-channel interference). Term $I_{b,l}$ is the interference power caused at the transmitter due to the baseband CF-based PAPR reduction and signal distortion at the power amplifier. The $\text{SNR}_{b,l} = S_{b,l}/N_0$ can be measured at the receiver using the reference signal and feedback to the transmitter. The problem is $\text{ISR}_{b,l} = I_{b,l}/S_{b,l}$. AMC needs the $\text{ISR}_{b,l}$ value for MCS selection before the PAPR reduction and power amplification. However, the exact $\text{ISR}_{b,l}$ value is surely dependent on the selected MCS.

We apply a lookup table-based prediction of $\text{ISR}_{b,l}$. Fig. 2 shows the proposed AMC with interference prediction. Based on a previously performed computer simulation, we note that the mean value of $\text{ISR}_{b,l}$ is largely dependent on the clipping threshold, P_{th} , at the baseband PAPR reduction, the IBO at the power amplifier, frequency block index b , stream index l , and $\text{SNR}_{b,l}$ ($\text{SNR}_{b,l}$ affects the waterfilling-based power allocation). Therefore, the lookup table forms $\text{ISR}(P_{th}, \text{IBO}, b, l, \text{SNR})$. Based on the predicted $\text{SNR}_{b,l}$, the set of the modulation scheme, $m_{b,l}$, and code rate, $R_{b,l}$, is selected that maximizes the throughput.

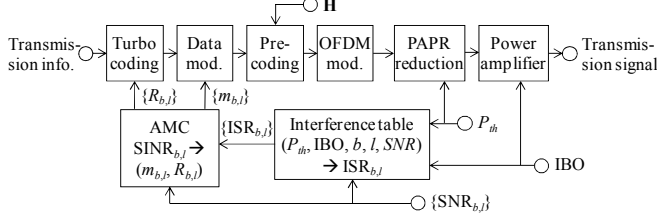


Figure 2. Proposed AMC with interference power prediction.

IV. NUMERICAL RESULTS

Table I gives the simulation parameters. In AMC, the modulation level is selected from QPSK to 256QAM. A rate-1/3 turbo code is used and a higher coding rate is obtained by puncturing. We compare the proposed method to the conventional iterative CF method. The AMC using the lookup-table-based prediction of SINR after PAPR reduction is applied to the conventional CF as well as the proposed method. To evaluate the sufficiently converged performance, the number of iterations in the PAPR reduction process is set to 10 for both the proposed and conventional methods. Term P_{th} is defined as the signal power threshold normalized by the signal power per antenna averaged over the channel realizations.

TABLE I. SIMULATION PARAMETERS

Total number of subcarriers, BK	512
Number of FFT points, F	4096
Number of frequency blocks, B	8
Number of transmitter antennas, N_{tx}	4, 6
Number of receiver antennas, N_{rx}	4
Data modulation, m	QPSK, 8PSK, 16QAM, 64QAM, 256QAM
Channel coding	Turbo code (Mother code rate = 1/3)
SNR	20 dB
Channel model	Block Rayleigh i.i.d. among antennas and frequency blocks
Number of iterations in PAPR reduction	10

Fig. 3 shows the signal power spectral density (PSD) at the power amplifier output. Overall transmission bandwidth W is defined as the sum of the effective bandwidth for BK subcarriers and the guard bandwidth, which equals 1/9 of the effective bandwidth, according to the LTE specifications [22]. Fig. 3 shows that the shape of the PSD for the proposed method is almost identical to that for the conventional method assuming appropriate P_{th} and IBO parameters. In the following, we use the ACLR [22] as a metric for out-band radiation.

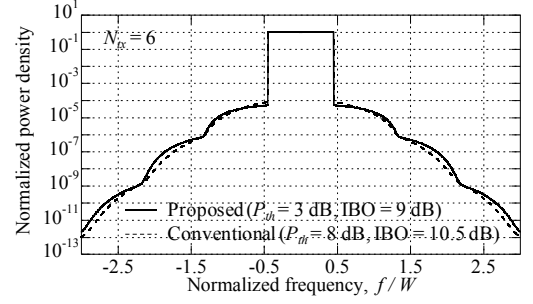
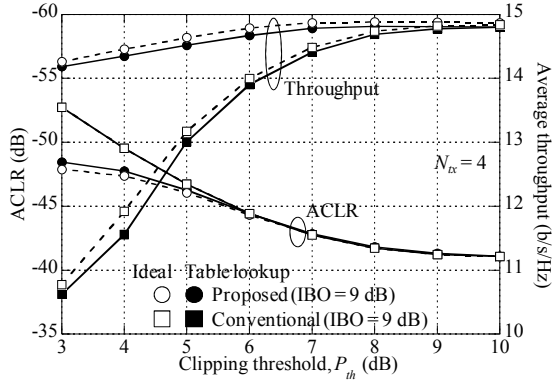


Figure 3. Signal PSD at the power amplifier output ($N_{tx} = 6$).

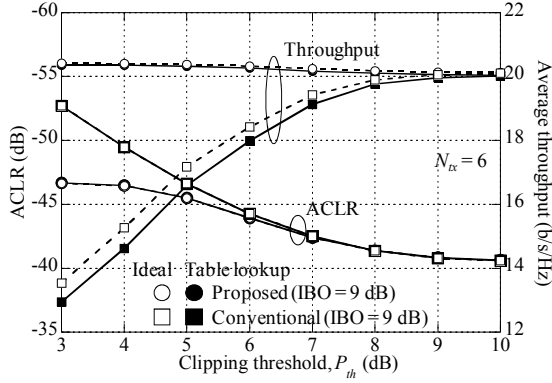
Figs. 4(a) and 4(b) show the ACLR and average throughput as a function of P_{th} for N_{tx} of 4 and 6, respectively. The IBO is set to 9 dB. We also plot the performance assuming ideal $\text{ISR}_{b,l}$ estimation in AMC for comparison. The proposed AMC using a lookup table for the ISR works well since the performance gap compared to the ideal case is small. The performance gap of the proposed PAPR reduction method is smaller than that for the conventional CF, since the interference power is concentrated on the most inefficient streams in the proposed method. In the conventional CF, the ACLR decreases as P_{th} decreases since the PAPR of the input signal to the power amplifier decreases. Although the same tendency is observed in the proposed method, the ACLR value at the given P_{th} of the proposed method is higher than that for the conventional CF. This is due to the deteriorated PAPR reduction capability using a limited number of streams in the proposed method. Meanwhile, the throughput of the conventional CF is significantly reduced as P_{th} decreases due to severe interference caused by clipping. This degradation is very small in the proposed method thanks to the decreased interference power to the streams with high singular values. When N_{tx} is 6, the average throughput is maximized for the P_{th} of 3 dB. This is because the proposed method does not impart interference to the effective data streams at the baseband PAPR reduction in this case ($N_{tx} > N_{rx}$), and the reduced PAPR results in reduced signal distortion at the power amplifier.

Fig. 5 shows the ACLR and average throughput as a function of the IBO for N_{tx} of 6. As the IBO increases, the ACLR decreases. The average throughput is increased by increasing the IBO from 4 dB due to the increase in the output power. However, as we increase the IBO further, the throughput tends to decrease due to signal distortion. Therefore, choosing an appropriate set of P_{th} and IBO is important.

Finally, Fig. 6 shows the average throughput as a function of the ACLR. For the respective PAPR reduction methods, the set of P_{th} and IBO is controlled so that the average throughput is maximized for a given ACLR. The figure shows that the proposed method is effective in increasing the throughput compared to the conventional CF especially when the required ACLR value is low. The figure also shows that the effectiveness of the proposed method is increased as N_{tx} increases. For example, when N_{tx} is 6, the proposed method increases the average throughput by approximately 1.9 b/s/Hz compared to the conventional CF at the ACLR of -45 dB, which is a requirement for LTE [22].



(a) $N_{tx} = 4$



(b) $N_{tx} = 6$

Figure 4. ACLR and average throughput as a function of P_{th} .

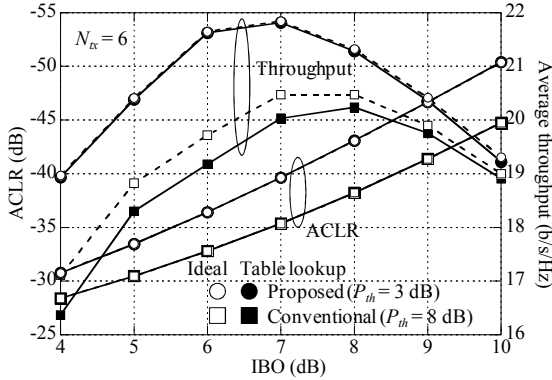


Figure 5. ACLR and average throughput as a function of IBO ($N_{tx} = 6$).

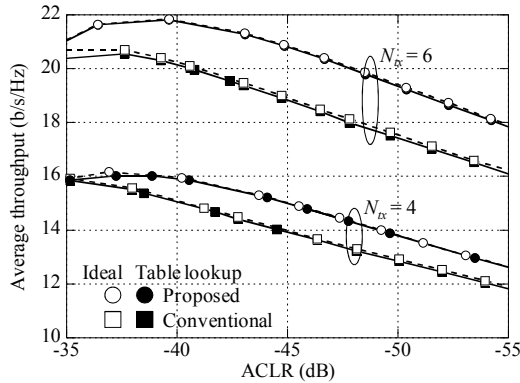


Figure 6. Average throughput as a function of ACLR.

V. CONCLUSION

This paper proposed the enhancement to our previously reported adaptive PAPR reduction method based on CF for eigenmode MIMO-OFDM signals. We enhanced the method to accommodate the case with AMC. Since the PAPR reduction process incurs interference, AMC should take into account this degradation before PAPR reduction for accurate selection of the MCS for each spatial stream. We use a lookup table-based prediction of the SINR after PAPR reduction, in which the interference caused by the PAPR reduction is obtained as a function of the stream index, frequency block index, clipping threshold for PAPR reduction, and IBO of the power amplifier. The simulation results show that the proposed PAPR reduction method increases the average throughput compared to the conventional CF method for a given ACLR assuming the Rapp model as an AM-AM conversion of the power amplifier. For example, when N_{tx} is 6 and the SNR is 20 dB, the proposed method increases the average throughput by approximately 1.9 b/s/Hz compared to the conventional CF at the ACLR of -45 dB, which is a requirement for LTE.

REFERENCES

- [1] 3GPP TS36.300, Evolved Universal Terrestrial Radio Access (E-UTRA) and Evolved Universal Terrestrial Radio Access Network (E-UTRAN); Overall description.
- [2] G. G. Raleigh and J. M. Cioffi, "Spatio-temporal coding for wireless communication," *IEEE Trans. Commun.*, vol. 46, no. 3, pp. 357-366, Mar. 1998.
- [3] S. H. Han and J. H. Lee, "An overview of peak-to-average power ratio reduction techniques for multicarrier transmission," *IEEE Wireless Communications*, vol. 12, no. 2, pp. 56-65, Apr. 2005.
- [4] X. Li and L. J. Cimini, Jr., "Effect of clipping and filtering on the performance of OFDM," *IEEE Commun. Lett.*, vol. 2, no. 5, pp. 131-133, May 1998.
- [5] J. Armstrong, "Peak-to-average power reduction for OFDM by repeated clipping and frequency domain filtering," *Elect. Lett.*, vol. 38, no. 8, pp. 246-247, Feb. 2002.
- [6] B. S. Krongold and D. L. Jones, "PAR reduction in OFDM via active constellation extension," *IEEE Trans. Broadcast.*, vol. 49, no. 3, pp. 258-268, Sep. 2003.
- [7] A. Aggarwal and T. H. Meng, "Minimizing the peak-to-average power ratio of OFDM signals using convex optimization," *IEEE Trans. Sig. Proc.*, vol. 54, no. 8, pp. 3099-3110, Aug. 2006.
- [8] J. Tellado and J. M. Cioffi, "Efficient algorithms for reducing PAR in multicarrier systems," in *Proc. IEEE Int. Symp. Inf. Theory*, p. 191, Cambridge, MA, Aug. 1998.
- [9] H. Ando and K. Higuchi, "Comparison of PAPR reduction methods for OFDM signal with channel coding," in *Proc. IEEE APWCS2009*, Seoul, Korea, Aug. 2009.
- [10] H. Lee, D. N. Liu, W. Zhu, and M. P. Fitz, "Peak power reduction using a unitary rotation in multiple transmit antennas," in *Proc. IEEE ICC2005*, pp. 2407-2411, Seoul, Korea, May 2005.
- [11] G. R. Woo and D. L. Jones, "Peak power reduction in MIMO OFDM via active channel extension," in *Proc. IEEE ICC2005*, pp. 2636-2639, Seoul, Korea, May 2005.
- [12] S. Suyama, H. Adachi, H. Suzuki, and K. Fukawa, "PAPR reduction methods for eigenmode MIMO-OFDM transmission," in *Proc. IEEE VTC2009-Spring*, Barcelona, Spain, Apr. 2009.
- [13] R. W. Bauml, R. F. H. Fischer, and J. B. Huber, "Reducing the peak-to-average power ratio of multicarrier modulation by selected mapping," *Electron. Lett.*, vol. 32, no. 22, pp. 2056-2057, Oct. 1996.
- [14] S. H. Muller and J. B. Huber, "OFDM with reduced peak-to-average power ratio by optimum combination of partial transmit sequences," *Electron. Lett.*, vol. 33, no. 5, pp. 368-369, Feb. 1997.
- [15] M. Iwasaki and K. Higuchi, "Clipping and filtering-based PAPR reduction method for precoded OFDM-MIMO signals," in *Proc. IEEE VTC2010-Spring*, Taipei, Taiwan, May 2010.
- [16] Y. Sato, M. Iwasaki, and K. Higuchi, "CF-based adaptive PAPR reduction Method for precoded OFDM-MIMO signals in frequency-selective faded channel," in *Proc. IEEE VTC2010-Fall*, Ottawa, Canada, Sep. 2010.
- [17] D. P. Bertsekas, *Nonlinear Programming*, Athena Scientific, Belmont, U.S.A., 1999.
- [18] M. Sharif, M. Gharavi-Alkhansari, and B. H. Khalaj, "On the peak-to-average power of OFDM signals based on oversampling," *IEEE Trans. Commun.*, vol. 51, no. 1, pp. 72-78, Jan. 2003.
- [19] C. Rapp, "Effects of the HPA-nonlinearity on a 4-DPSK/OFDM signal for a digital sound broadcasting system," in *Proc. ECSC'91*, Luetich, Oct. 1991.
- [20] S. C. Thompson, J. G. Proakis, and J. R. Zeidler, "The effectiveness of signal clipping for PAPR and total degradation reduction in OFDM systems," in *Proc. IEEE Globecom 2005*.
- [21] E. Costa and S. Pupolin, "M-QAM-OFDM system performance in the presence of a nonlinear amplifier and phase noise," *IEEE Trans. Commun.*, vol. 50, no. 3, pp. 462-472, Mar. 2002.
- [22] 3GPP TS36.104, Evolved Universal Terrestrial Radio Access (E-UTRA); Base Station (BS) radio transmission and reception.